frontiers | Frontiers in Materials

ORIGINAL RESEARCH
published: 29 April 2022
doi: 10.3389/fmats.2022.847497

Preservation of Titanium in a Naringin-Containing Solution to Enhance Osteogenic and Anti-inflammatory Activities *In Vitro*

Wei Chen[1,2†], *Wen-qing Zhu*[1,2†], *Shan Su*[1,2], *Yao Liu*[1,2] *and Jing Qiu*[1,2,3*]

[1]Department of Oral Implantology, Affiliated Stomatological Hospital of Nanjing Medical University, Nanjing, China, [2]Jiangsu Province Key Laboratory of Oral Diseases, Nanjing, China, [3]Jiangsu Province Engineering Research Center of Stomatological Translational Medicine, Nanjing, China

When exposed to air, the titanium implants undergo changes in surface characteristics and biological activity, which is known as biological aging. It is important to find a suitable storage method to slow down the biological aging of titanium. The purpose of this study was to develop a naringin-containing storage solution and evaluate the effects of this storage method on physicochemical properties as well as osteogenic and anti-inflammatory activities of commercial pure titanium (cp-Ti) and sandblasted with large grit and acid-etched titanium (SLA-Ti). Titanium surfaces stored in air and 0.9% NaCl solution for 4 weeks were served as control, and samples submerged in three different concentrations of naringin-containing solution for 4 weeks were used to investigate the new storage method. Surface topography images showed that nanostructures were observed on liquid-stored SLA-Ti surfaces. The storage condition did not influence the roughness of both cp-Ti and SLA-Ti. However, the wettability of titanium varied with the storage methods. Titanium stored in the naringin-containing solution exhibited lower contact angles. Samples stored in aqueous solution were less susceptible to hydrocarbon contamination. The preservation of titanium in the 10 μM naringin-containing solution enhanced the adhesion, proliferaton, and differentiation of osteoblasts. In addition, macrophages on samples stored in 10 μM and 100 μM naringin-containing solutions displayed better anti-inflammatory effect. In summary, the 10 μM naringin-containing solution could enhance osteogenic and anti-inflammatory activities of titanium and was proved to be an effective new storage condition.

Keywords: titanium, naringin, storage solution, osteogenic, anti-inflammatory

OPEN ACCESS

Edited by:
Ayşen Tezcaner,
Middle East Technical University, Turkey

Reviewed by:
Guya Diletta Marconi,
University of Studies G. d'Annunzio Chieti and Pescara, Italy
Ahmet Engin Pazarçeviren,
Middle East Technical University, Turkey

****Correspondence:***
Jing Qiu
qiujing@njmu.edu.cn

†These authors have contributed equally to this work

Specialty section:
This article was submitted to Biomaterials, a section of the journal Frontiers in Materials

Received: *02 January 2022*
Accepted: *22 March 2022*
Published: *29 April 2022*

Citation:
Chen W, Zhu W-q, Su S, Liu Y and Qiu J (2022) Preservation of Titanium in a Naringin-Containing Solution to Enhance Osteogenic and Anti-inflammatory Activities In Vitro. Front. Mater. 9:847497. doi: 10.3389/fmats.2022.847497

INTRODUCTION

Implant denture has gradually become an ideal treatment for many patients with dentition defects due to its features of comfort, high chewing efficiency, and long-term stability (Mijiritsky et al., 2015). Pure titanium and titanium alloys have been widely used in the field of oral implants because of their excellent biocompatibility and strong mechanical properties (Prasad et al., 2015; Marconi et al., 2020). The surface characteristics and biological properties of dental implants are closely related to the speed and strength of osteointegration (Bosshardt et al., 2017; Marconi et al., 2020; Marconi et al., 2021).

After preparation, implants need to be stored for a period through transportation, sales, and other links before clinical practice. Recent studies discovered that long-term storage of titanium in the air will cause aging (Lee and Ogawa, 2012). The aging phenomenon of titanium is related to the hydrocarbon adsorbed by titanium implants in the air (Att et al., 2009a; Att et al., 2009b). The continuous accumulation of these hydrocarbons will lead to changes in the physiochemical properties of the titanium surface such as the increase of contact angle and the decrease of protein adsorption capacity, which will adversely affect the biological performance of the implant (Hori et al., 2009; Att and Ogawa, 2012; Lu et al., 2012). The adhesion and proliferation of osteoblasts on the titanium surface were significantly decreased after 4 weeks of preservation in a sealed container. *In vivo* studies, the bone-implant contact percentages and the strength of osteointegration of the 4-week-old implant were less than 50% of the control group (Att et al., 2009b). This phenomenon is known as the biological aging of titanium (Minamikawa et al., 2016). It has been proved that the aging of titanium can occur on various modified titanium surfaces (Att et al., 2009b; Hori et al., 2009).

In addition, physicochemical changes may lead to different responses of macrophages (Hamlet et al., 2012). Polarized macrophages can be divided into two phenotypes: the classical pro-inflammatory (M1) and the alternative anti-inflammatory (M2). M1 and M2 macrophages can transform into each other under certain conditions. The shift from an M1 to an M2 phenotype plays an important role in promoting tissue healing and regeneration (Ping et al., 2021). Different phenotypes of macrophages secrete different anti-/pro-inflammatory factors forming various immune microenvironments. The immune and skeletal systems share the same microenvironment, therefore, the interaction between immune and skeletal systems is crucial for osteointegration (Chen Z. et al., 2016).

At present, the conventional storage method of the implant is to be sealed under normal temperature and pressure. This kind of gas-permeable packaging makes the implant vulnerable to hydrocarbon contamination in the air (Kasemo and Lausmaa, 1988). Studies have shown that there are different degrees of hydrocarbon pollution on the surface of commercial implants used in clinics (Massaro et al., 2002; Aita et al., 2009). In order to keep the physicochemical properties and biological characteristics of titanium implants stable during storage, many scholars have conducted in-depth research on the anti-aging methods of titanium implants in recent years. Various methods have been reported to delay the aging of titanium implants, such as ultraviolet radiation (Suzuki et al., 2009), wet storage (Wennerberg et al., 2013), inert gas storage (Zhao et al., 2015), etc. Among them, the biological activity on the surface of titanium could not last for a long time after ultraviolet exposure (Choi et al., 2017); gas storage required more complex and expensive packaging technology; the wet storage method is simple and easy to operate, which can keep the surface of the implant hydrophilic and prevent the direct pollution of the titanium surface from hydrocarbons in the air (Lu et al., 2012). It has been proved that titanium surfaces preserved in saline can promote bone-implant contact percentages and decrease the secretion of inflammatory cytokines (Buser et al., 2004; Lotz et al., 2017). The saline storage method has been gradually applied in the clinic (Lotz et al., 2017).

Naringin is a kind of flavonoid that has been widely used in traditional Chinese medicine. It has many biological activities and pharmacological effects (Chen R. et al., 2016). Naringin has been commonly used in the treatment of fracture healing and osteoporosis due to its ability to enhance bone density and reduce bone loss (Lavrador et al., 2018). In addition, naringin has anti-inflammatory properties (Alam et al., 2014). It has been proved that naringin can decrease serum concentrations of inflammatory factors in animal models. The NF-κB signal pathway plays an important role in the anti-inflammatory effects of naringin (Miles and Calder, 2021).In this study, naringin has been used in surface modification of titanium (Yu et al., 2017; Shen et al., 2021).

So far, the preservation fluids commonly used for wet storage in studies are mostly double-distilled water or saline. Naringin has never been added into the liquid for implant storage. The purpose of this study was to develop an effective and economic wet storage method. We used different concentrations of naringin-containing solution for implant storage to study the effects of this storage method on the anti-aging of implant surfaces, and find out the optimal concentration for implant preservation. In addition, we assessed the anti-inflammatory effects of titanium after soaking in a naringin-containing solution and potential signaling pathways in macrophages. Commercial pure titanium (cp-Ti) and sandblasted with large grit and acid-etched titanium (SLA-Ti) were tested in this study.

MATERIALS AND METHODS

Preparation of Storage Solution and Titanium Surfaces

Preparation of storage solution containing naringin: 0.9% NaCl solution (AR, SCR, China) and naringin (purity≧98%, Sigma, Shanghai, China) were purchased for the preparation of storage solution configuration. First, 0.583 g of naringin crystals were weighed and dissolved in 1 L 0.9% NaCl solution. After stirring repeatedly and standing for full mixing, 1 mM naringin-containing solution was obtained. 1 mM naringin-containing solution was diluted 10 times and 100 times, respectively with 0.9% NaCl solution to prepare 100 and 10 μM naringin-containing storage solutions. All solutions were filtered through a 0.22 μm pore size filter (Kurabo, Osaka, Japan) in a sterile air cabinet before use.

Preparation of titanium surfaces: commercially pure titanium (99.5 wt% purity, Baoji Titanium, China) disks with dimensions of Φ5 mm × 1 mm and Φ30 mm × 1 mm were polished with a series of SiC sandpapers (180, 400, 600, 1,200, and 1,500 grit) as cp-Ti. The SLA titanium surfaces, denoted as SLA-Ti samples, were obtained after being sandblasted with Al_2O_3, followed by etching with a solution containing HF/HNO_3 (at room temperature, for 10 min) and a solution containing H_2SO_4/HCl (at 80°C in a water bath, for 30 min). The two kinds of titanium surfaces were ultrasonically cleaned in anhydrous ethanol and deionized water for 10 min, and

then autoclaved at 121°C for 15 min prior to use. Finally, the two kinds of newly prepared specimens were stored in air, 0.9% NaCl solution, 10 μM, 100 μM, and 1 mM naringin-containing solution and were preserved in a sealed container for 4 weeks at ambient temperature.

Surface Characterization

The surface morphology of titanium disks, which were stored in different media for 4 weeks, was observed using a scanning electron microscope (SEM, MAIA3 RISE, TESCAN, Czech) under the accelerating voltage of 10.0 kV and the working distance of 5 mm. Raman spectral data were recorded by using a Tescan-WITec RISE microscope (TESCAN, Czech). This system contained the WITec Confocal Raman Imaging System (WITec, Ulm, Germany), which is equipped with a 532 nm excitation of an Nd:YAG laser and a 20X, NA = 0.4, objective lens. The integration time of Raman spectra was 0.2 s. The roughness of samples was examined by using an optical profilometer (MicroXamTM, Phase-Shift, UP, Rtec co, United States). The surface elemental compositions were detected by the X-ray photoelectron spectroscopy (XPS, Thermo Scientific Escalab 250Xi, United States) under vacuum conditions. The wettability of samples under different storage conditions was tested by using a standard optical contact angle instrument (SL200B, Kono, United States) using the liquid drop method. A droplet of 2 μL of sessile distilled water was dropped onto the surface in an ambient environment and the contact angles were measured using a standard optical contact angle meter. All tests were conducted in triplicate.

Cell Culture

MC3T3-E1 cells, an osteoblast-like cell line, were purchased from the Chinese Academy of Sciences Cell Bank (Shanghai, China). The cells were incubated in α-Minimum Essential Medium (α-MEM; Gibco, United States) containing 10% fetal bovine serum (FBS; Gibco, United States) and 1% penicillin/streptomycin (Gibco, United States). RAW264.7 cells, a murine macrophage-like cell line, were purchased from the Chinese Academy of Sciences Cell Bank (Shanghai, China). The cells were cultured in Dulbecco's Modified Eagle's Medium (DMEM, Gibco, United States) containing 10% fetal bovine serum and 1% penicillin/streptomycin. MC3T3-E1 cells and RAW264.7 cells were incubated in a humidified atmosphere of 5% CO_2 and 95% air at 37°C. The culture medium was refreshed every 2 days. Cells were passaged when cell confluence was up to 80%.

Cell Adhesion Assay

MC3T3-E1 cells (4×10^3 cells per well) were seeded on the surface of the specimen in 96-well plates. After culturing for 4 h, cells were fixed with 4% paraformaldehyde at room temperature for 10 min. Afterward, each sample was stained with Rhodamine Phalloidin (Cytoskeleton, United States) for 30 min in the dark and then stained with 4′,6-diamidino-2-phenylindole (DAPI) (Beyotime, Shanghai, China) for 60 s. The cell adhesion and spreading morphology were observed at 400× magnification using a laser scanning confocal microscope (LSM710, Zeiss, GER). All tests were repeated in triplicate.

TABLE 1 | Primer sequences of target genes for real-time quantitative polymerase chain reaction (RT-qPCR) in this study.

Gene		Primer sequence (5′-3′)
Runx2	F	CCGAAATGCCTCCGCTGTTATG
	R	TCTGTCTGTGCCTTCTTGGTTCC
OSX	F	AGTTCACCTGCCTGCTCTGTTC
	R	GCGGCTGATTGGCTTCTTCTTC
OCN	F	CAAGCAGGAGGGCAATAAGGTAGTG
	R	CATACTGGTCTGATAGCTCGTCACAAG
IL-1β	F	ACCTCACAAGCAGAGCACAAGC
	R	AGACACGGATTCCATGGTGAAGTC
IL-6	F	CCACTTCACAAGTCGGAGGC
	R	TCTGCAAGTGCATCATCGTTGT
IL-4	F	TACCAGGAGCCATATCCACGGATG
	R	TGTGGTGTTCTTCGTTGCTGTGAG
IL-10	F	ACATACTGCTAACCGACTCCTTAATGC
	R	CTTCACCTGCTCCACTGCCTTG
GAPDH	F	GCTCTCCAGAACATCATCC
	R	TGCTTCACCACCTTCTTG

Cell Proliferation Assay

Cell proliferation assay was performed on day 1, day 3, and day 7 using the CCK-8 kit (Beyotime, Shanghai, China). MC3T3-E1 cells (2×10^3 cells per well) were seeded on the surface of the specimen after 4 weeks of storage under various conditions in 96-well plates. After incubating cells for 1, 3, and 7 days, the medium of each well was refreshed with 100 μL of fresh medium containing 10 μL of CCK-8 reagent, and then incubated at 37°C for another 2 h. The absorbance of the medium was measured at 450 nm wavelength with a microplate reader (Spectramax190, CA, United States). The experiment was performed four times.

Western Blotting

MC3T3-E1 cells (2×10^5 cells per well) and RAW264.7 cells (2×10^5 cells per well) were seeded in six-well plates, respectively. After 7 days' culture of MC3T3-E1 cells and 3 days' culture of RAW264.7 cells, they were washed with cold PBS and total protein samples were extracted using RIPA buffer. Protein concentrations of samples were determined using a BCA protein assay kit (KeyGen, Biotech, Nanjing, China). After the electrophoresis, protein extract samples (20 μg) were separated and then were transferred to polyvinylidene fluoride (PVDF) membranes (Millipore, United States).The membranes were blocked with 5% skimmed milk at room temperature for 1 h and then incubated with primary antibodies against Runx2 (12,556; CST, United States), osteocalcin (OCN; ab10911, EMD Millipore, United States), Osterix (OSX; ab22552; Abcam, United States), IL-1β (31202S, CST, United States), IL-6 (12912S, CST, United States), p65 (8242S, CST, United States), p-p65(3033S, CST, United States), IκBα (4812S, CST, United States), p-IκBα (2859S, CST, United States), or GAPDH (60,004, Proteintech, United States) overnight at 4°C. These membranes were then incubated for 1 h with secondary antibodies (ZB-2301 and Goat anti-Rabbit IgG, ZSGB-BIO, China; AP124P and Goat anti-Mouse IgG, Millipore, United States). The protein levels were visualized by ECL

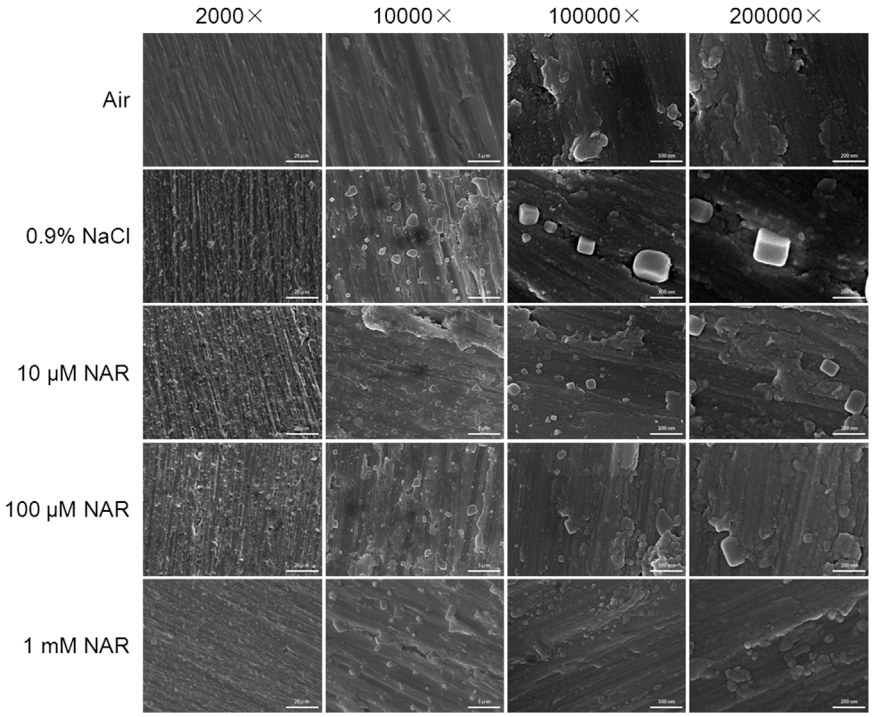

FIGURE 1 | Scanning electron microscopy images of surface morphology of cp-Ti under different storage conditions for 4 weeks. (Magnification 2000×, 10,000×, 100,000× and 200,000×).

detection (Thermo Fisher Scientific). GAPDH was used as an internal control. The experiments were repeated in triplicate.

RNA Isolation and Real-Time Quantitative PCR Analysis

RNA was extracted from cells using the TRIzol reagent (Invitrogen, CA, United States) and was reverse transcribed into complementary DNA (cDNA) using the PrimeScript RT Reagent Kit (Takara Bio, Kusatsu, Japan). Real-time quantitative PCR analyses were performed using the SYBR Premix Ex Taq (Takara, Kusatsu, Japan) and detected using the QuantStudio 7 Flex Real-Time PCR System (Thermo Fisher Scientific, Waltham, MA, United States). The primer sequences are listed in **Table 1**. The values used GAPDH for normalization, and the $2^{-\Delta\Delta Ct}$ equation was used to calculate the relative quantification of gene expression. All acquired data using RT-qPCR came from multiple experiments with three independent samples.

Osteogenic Differentiation Effect of MC3T3-E1 Cells in Conditioned Medium

RAW264.7 cells (2×10^5 cells per well) were seeded in different groups described above. After incubating for 3 days in DMEM, the culture medium of each group was collected and centrifuged (1,000 rpm, 5 min, 4°C), then filtered through a 0.22 μm pore size filter (Kurabo, Osaka, Japan) to remove cell debris. The collected supernatant was mixed with α-MEM containing 10% FBS and 1% penicillin/streptomycin at a ratio of 1:4 to get a conditioned medium (CM). CM was placed at −80°C for later use. MC3T3-E1 cells (2×10^5 cells/well) were seeded in six-well plates and cultured with CM. The expression of target osteogenic genes (Runx2, OSX, OCN) was measured by Western blot.

Statistical Analysis

The collected data were analyzed using SPSS 22.0 software (SPSS, Inc., Chicago, IL, United States). Multiple comparisons were performed by a one-way analysis of variance (ANOVA) followed by the Student–Newman–Keuls (S-N-K) method. When $p < 0.05$, the difference was considered statistically significant.

RESULTS

Surface Characteristics

The surface topography of samples under different storage conditions is shown in **Figures 1**, **2**. Neat mechanical scratches on cp-Ti and uniform micro-scale pits on SLA-Ti were revealed on SEM images under low magnifications. However, high magnification of SEM images revealed that nanoparticles could be observed only on SLA-Ti stored in solution, whereas no specific changes were observed for cp-Ti and SLA-Ti stored dry. Titanium samples under 0.9% NaCl solution and 0.9% NaCl solution containing different concentrations of naringin exhibited crystals on their surfaces.

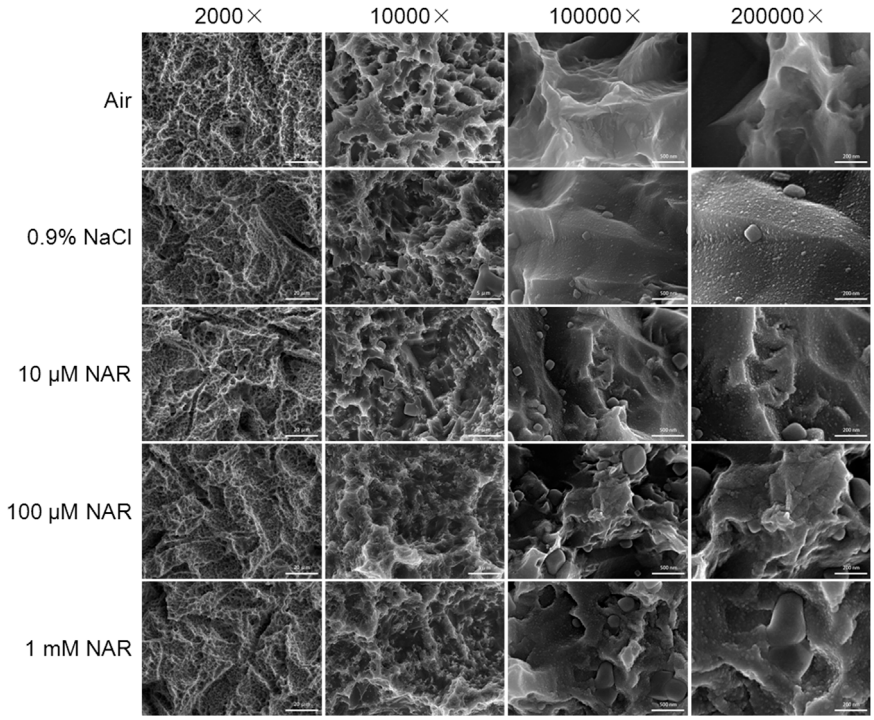

FIGURE 2 | Scanning electron microscopy images of surface morphology of SLA-Ti under different storage conditions for 4 weeks. (Magnification 2000×, 100,00×, 1,000,00× and 2,000,00×).

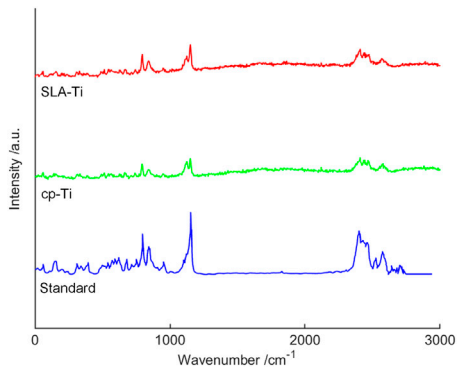

FIGURE 3 | Raman spectra of 1 mM naringin stored cp-Ti and SLA-Ti after 4 weeks and naringin Raman standard spectra.

Due to the limitation of detection accuracy, 1 mM naringin-containing solution stored cp-Ti and SLA-Ti were selected for the Raman test. **Figure 3** displayed that the obtained Raman spectra corresponded to the Raman standard map of naringin in the ST Japan Raman Database, their special characteristic peak Raman bands are overlapped. Topographical analysis demonstrated that cp-Ti and SLA-Ti surfaces had similar roughness, respectively, and the differences were not statistically significant (**Figure 4**).

The XPS analysis indicated the main chemical element on cp-Ti and SLA-Ti under different storage conditions (**Figure 5**; **Tables 1**, **2**). **Tables 2**, **3** displayed the quantitative atomic concentrations of cp-Ti and SLA-Ti under different storage conditions. **Figure 5** showed the wide scan spectrum of different samples. The quantified atomic ratios of Ti/C and O/C were given to evaluate carbon amounts between different groups. Results showed that titanium surfaces stored in air exhibited the highest carbon content. Titanium preserved in 0.9% NaCl or 10 μM naringin-containing solution suffered the lowest carbon contamination. The carbon levels of titanium disks soaked in 100 μM and 1 mM naringin-containing solution increased gradually. It may contribute to the naringin crystals adsorbed on the titanium surface that increase with the concentration of naringin-containing solution. The result demonstrated that titanium implants preserved in aqueous solution could reduce carbon pollution from the air.

The surface contact angles of two kinds of titanium surfaces under different storage methods are shown in **Figure 6**. The cp-Ti and SLA-Ti stored in air showed hydrophobicity. The titanium surfaces preserved in 0.9% NaCl solution showed lower contact angles. Samples stored in the naringin-containing solution exhibited superhydrophilicity compared with other storage methods. The result revealed that the hydrophilic property of the titanium preserved in the naringin-containing solution could be significantly enhanced.

Cell Adhesion

After incubating MC3T3-E1 cells for 4 h, **Figure 7** shows differences in cell morphology on cp-Ti and SLA-Ti preserved in different storage conditions. Compared with samples exposed

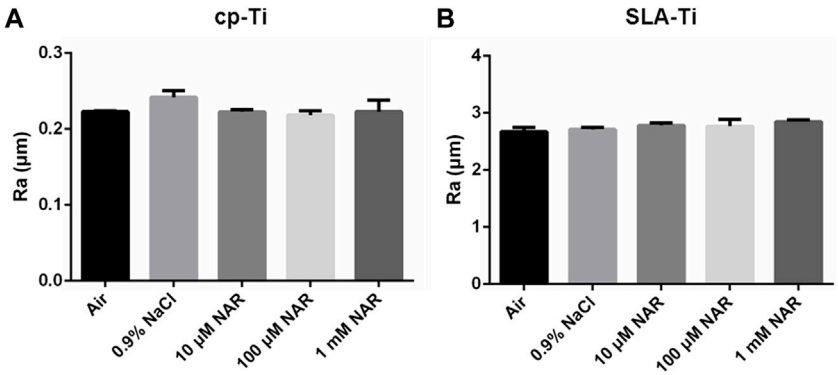

FIGURE 4 | Surface roughness of titanium surfaces under different storage conditions for 4 weeks. **(A)** cp-Ti; **(B)** SLA-Ti. Data are presented as means ± SD.

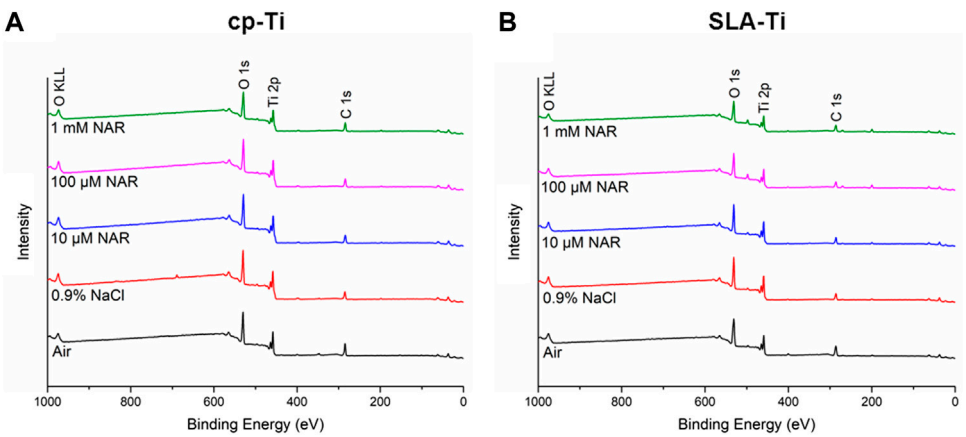

FIGURE 5 | XPS wide scan spectra analysis of titanium surfaces under different storage conditions for 4 weeks. **(A)** cp-Ti; **(B)** SLA-Ti.

TABLE 2 | Elemental compositions of cp-Ti samples detected by XPS.

Samples	Element composition (%)			Element ratio	
	O	Ti	C	O/C	Ti/C
Air	44.81	14.56	40.63	1.103	0.358
0.9% NaCl	49.64	22.35	28.01	1.772	0.798
10 μM NAR	48.09	21.51	30.39	1.582	0.708
100 μM NAR	48.68	19.76	31.56	1.542	0.626
1 mM NAR	45.56	17.08	37.35	1.220	0.457

TABLE 3 | Elemental compositions of SLA-Ti samples detected by XPS.

Samples	Element composition (%)			Element ratio	
	O	Ti	C	O/C	Ti/C
Air	42.14	16.24	41.62	1.012	0.390
0.9% NaCl	47.5	22.88	29.61	1.604	0.773
10 μM NAR	46.78	22.56	30.67	1.525	0.736
100 μM NAR	46.98	21.8	31.22	1.505	0.698
1 mM NAR	43.79	19.27	36.94	1.185	0.522

in the air, the cells on other titanium surfaces extended more pseudopodia. Cells on titanium surfaces preserved in 10 μM naringin-containing solution exhibited best morphology with the most evenly spread pseudopodia.

Cell Proliferation

Figure 8 displays the proliferation of MC3T3-E1 cells grown on titanium samples using different storage methods. After culturing for 1, 3, 7 days, the MC3T3-E1 cells proliferated on all the samples, however, there were no significant differences in the proliferation between different groups on day 1 and day 3. After incubating for 7 days, the cell proliferation on 10 μM naringin-containing solution stored cp-Ti was higher than in control groups. Moreover, the cell proliferation on 100 μM and 1 mM NAR groups of cp-Ti had no significant differences between the air group and 10 μM NAR group. On SLA-Ti surfaces, the cell proliferation of SLA-Ti preserved in the naringin-containing solution was higher than in the control group. It revealed that the three different concentrations of naringin-containing solution in the experiment formed a more appropriate environment for cell proliferation.

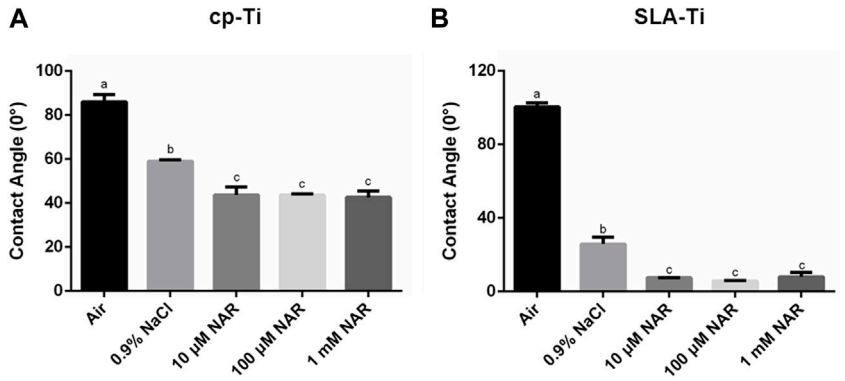

FIGURE 6 | Contact angles of titanium surfaces under different storage conditions for 4 weeks. **(A)** cp-Ti; **(B)** SLA-Ti. Data are presented as means ± SD, n = 3, bars with dissimilar letters indicate values that are significantly different from each other ($p < 0.05$).

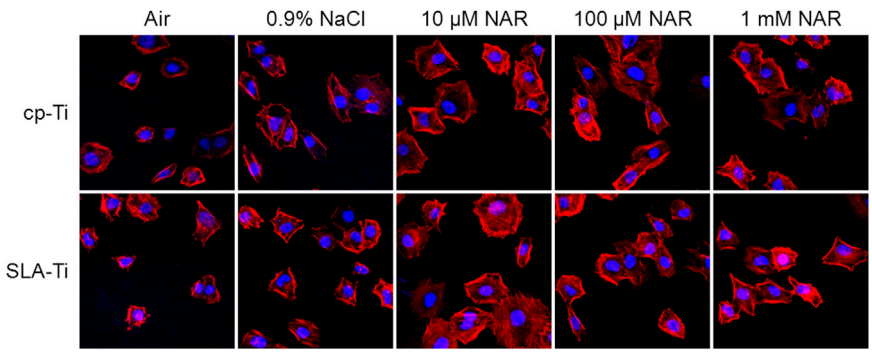

FIGURE 7 | Proliferation of MCETE-E1 cells cultured for 1, 3, and 7 days on different surfaces under different storage conditions for 4 weeks. **(A)** cp-Ti; **(B)** SLA-Ti. Data are presented as means ± SD, n = 4, bars with dissimilar letters indicate values that are significantly different from each other ($p < 0.05$).

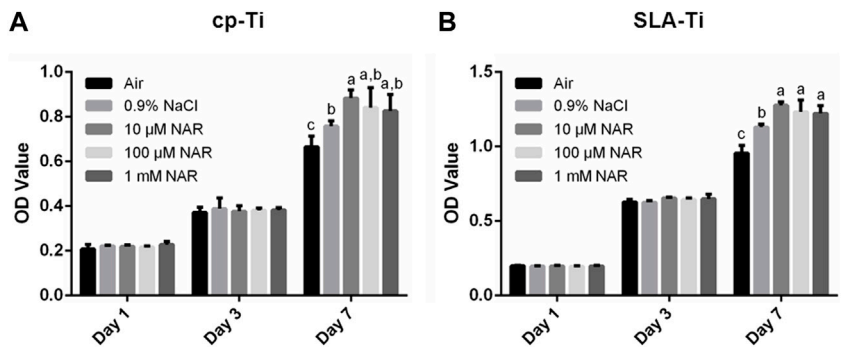

FIGURE 8 | LSCM images of MCETE-E1 cells cultured for 4 h on cp-Ti and SLA-Ti under different storage conditions for 4 weeks at 400× magnification.

Osteoblast Differentiation

Western blot analysis was used to determine the osteogenic related protein expression levels of MC3T3-E1 cells on titanium surfaces under various storage methods after culturing for 7 days. Runx2, OSX, and OCN were selected to evaluate the osteogenic capacity as significant osteogenic markers. Runx2 and OSX were markers of early stages of osteogenic differentiation and bone formation. OCN played an important role in the late stage of osteogenic differentiation and directly participated in the mineralization process (Tang Z. H. et al., 2021). As shown in **Figures 9A,B**, cells incubated on titanium surfaces preserved in naringin solution performed

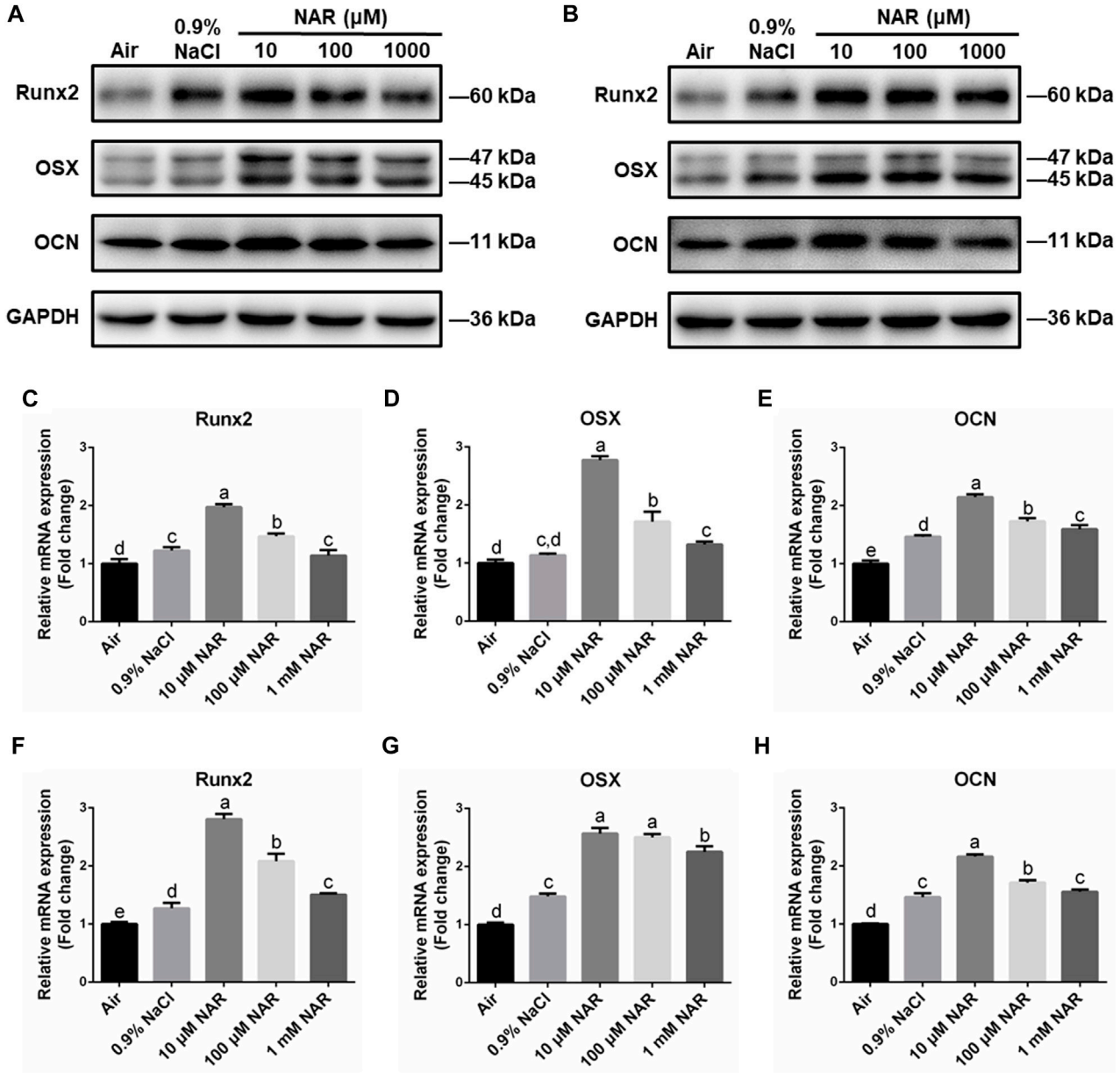

FIGURE 9 | Osteogenic differentiation ability of MC3T3-E1 cells on cp-Ti and SLA-Ti under different storage conditions for 4 weeks. **(A)** The protein expression of Runx2, OSX, and OCN on cp-Ti was analyzed by Western blot. **(B)** The protein expression of Runx2, OSX, and OCN on SLA-Ti was analyzed by Western blot. **(C–E)** The mRNA expression of Runx2, OSX, and OCN on cp-Ti was analyzed using real-time PCR. **(F–H)** The mRNA expression of Runx2, OSX, and OCN on SLA-Ti was analyzed using real-time PCR. Data are presented as means ± SD, n = 3, bars with dissimilar letters indicate values that are significantly different from each other ($p < 0.05$).

better osteogenic differentiation capacity compared with the air group and the 0.9% NaCl group. Moreover, cells on titanium samples stored in 10 μM naringin-containing solution expressed highest protein levels of Runx2, OSX, and OCN. The quantitative real-time PCR technique was used to assess the mRNA expressions of several osteogenic markers. As **Figures 9C–H** shows, consistent with the expressions of osteogenic proteins, cells on titanium disks preserved in 10 μM naringin-containing solution displayed the highest mRNA expressions of osteogenic related markers. The results reflected the good biocompatibilities of 10 μM naringin-containing solution stored in titanium.

Macrophage Response

The murine macrophage-like RAW264.7 cell line was selected as the *in vitro* model of macrophage response. To evaluate the effect of different storage modes on macrophage, RAW264.7 cells were incubated on the surface for 3 days, and the expressions of pro-inflammatory and anti-inflammatory related genes were detected. IL-1β and IL-6 were recognized to be associated with pro-

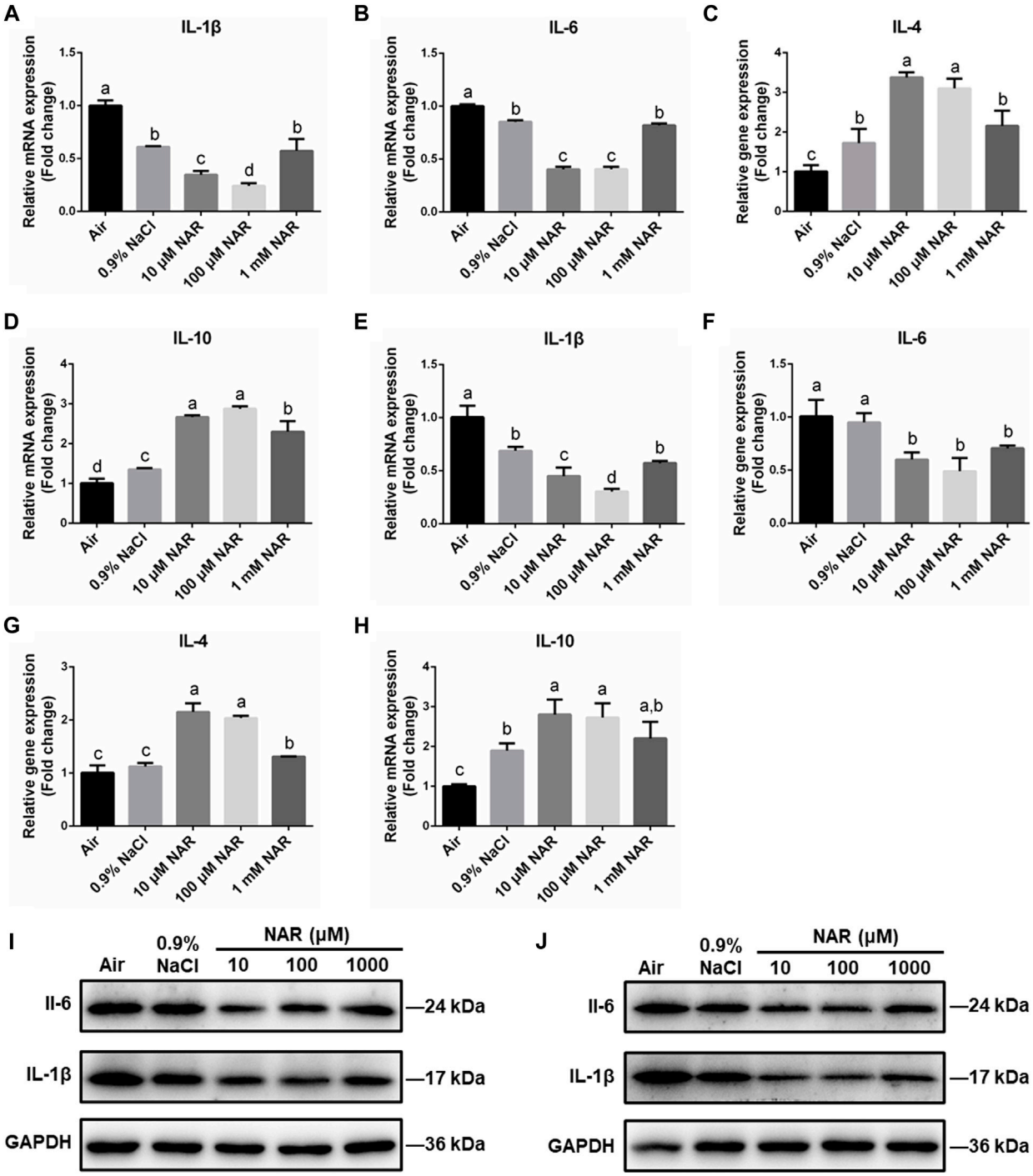

FIGURE 10 | Expression of pro-/anti-inflammatory factors of RAW264.7 cells on cp-Ti and SLA-Ti under different storage conditions for 4 weeks. **(A–D)** The mRNA expression of pro-/anti-inflammatory factors on cp-Ti was analyzed by real-time PCR. **(E–H)** The mRNA expression of pro-/anti-inflammatory factors on SLA-Ti was analyzed using real-time PCR. **(I)** The protein expression of IL-1β and IL-6 on cp-Ti was analyzed by Western blot. **(J)** The protein expression of IL-1β and IL-6 on SLA-Ti was analyzed by Western blot. Data are presented as means ± SD, n = 3, bars with dissimilar letters indicate values that are significantly different from each other ($p < 0.05$).

inflammation regulation, and IL-4 and IL-10 were anti-inflammatory related genes. As shown in **Figures 10A–H**, on cp-Ti and SLA-Ti surfaces, the expression levels of pro-inflammatory related genes in the 10 μM and 100 μM NAR groups were higher than in other groups. In contrast, the 10 μM and 100 μM NAR groups showed lower levels of the expression of IL-4 and IL-10 genes

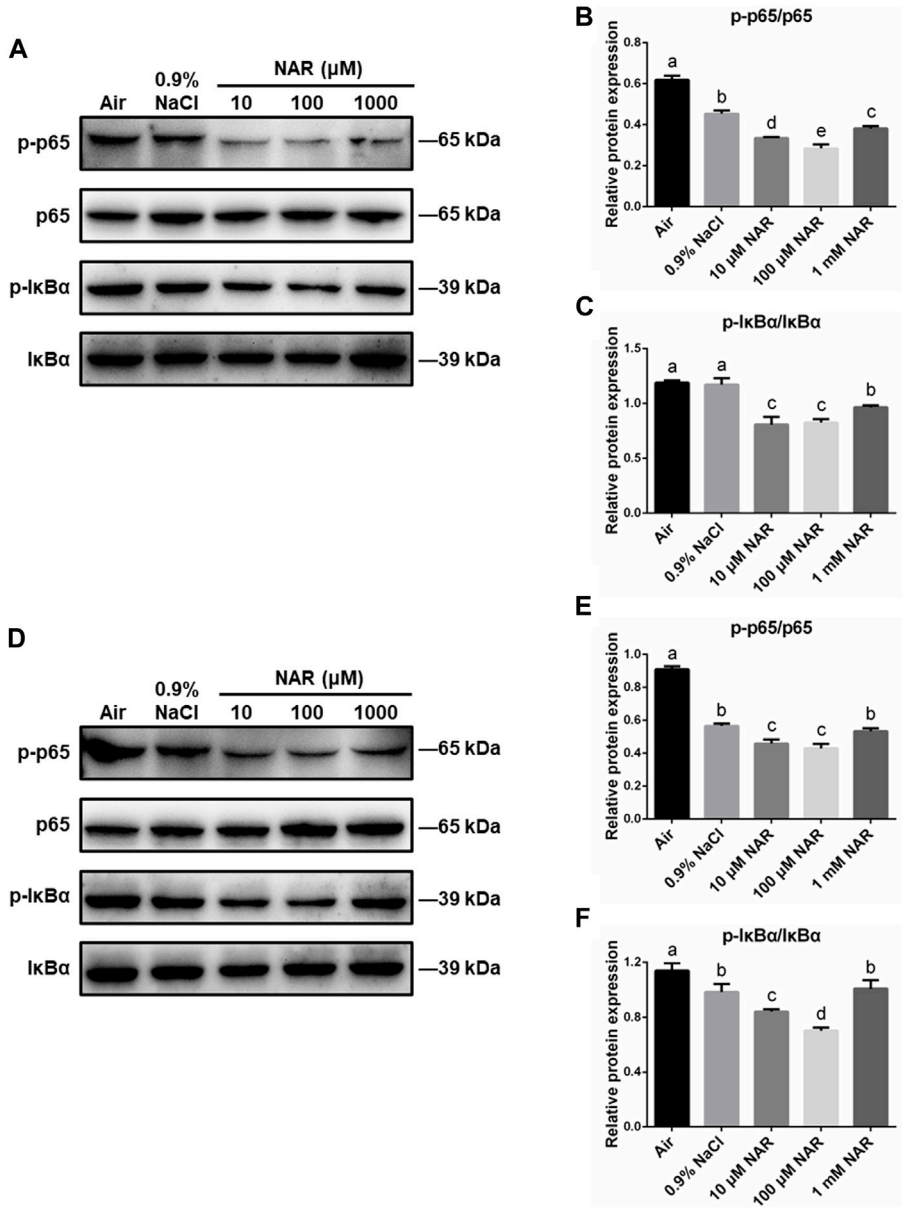

FIGURE 11 | The role of the NF-κB signal pathway of RAW264.7 cells on cp-Ti and SLA-Ti under different storage conditions for 4 weeks. **(A–C)** The essential proteins of the NF-κB signal pathway on cp-Ti were measured. **(D–F)** The essential proteins of the NF-κB signal pathway on SLA-Ti were measured. Data are presented as means ± SD, n = 3, bars with dissimilar letters indicate values that are significantly different from each other ($p < 0.05$).

compared to other groups. Western blot analysis was used to assess pro-inflammatory related protein expression levels. As **Figures 10I,J** showed, consistent with the expressions of pro-inflammatory related genes, cells on titanium disks stored in 10 and 100 μM naringin-containing solution displayed the better anti-inflammatory property.

Previous studies reported that the NF-κB signal pathway was associated with inflammatory responses, and naringin could antagonize the activation of the NF-κB signal pathway. Western blot was used to determine the expression levels of p-IκBα, IκBα, p-p65, and p65. **Figure 11** displays that 10 and 100 μM NAR groups performed lower expression of p-IκB and p-p65 while the levels of IκB, and p65 were largely unchanged among the five groups of cp-Ti and SLA-Ti. The results indicated that naringin may play an anti-inflammatory role at proper concentration.

The Assessment of Osteogenic Differentiation Ability in Conditioned Medium

In order to study the immunomodulatory effect of titanium samples under various storage conditions on osteogenic differentiation in MC3T3-E1 cells, the supernatants of

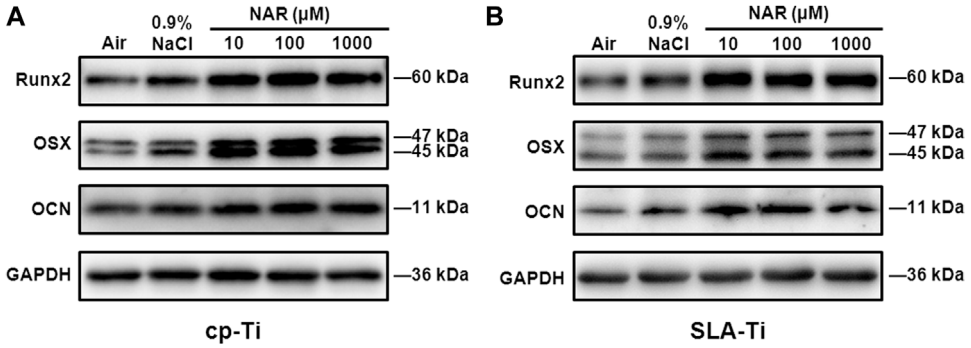

FIGURE 12 | Protein expression levels of osteogenic markers Runx2, OSX, and OCN of MC3T3-E1 cells in different CM of RAW264.7 cells on different surfaces under different storage conditions for 4 weeks. **(A)** cp-Ti; **(B)** SLA-Ti.

RAW264.7 cells were used as a conditioned medium. Western blot analysis was performed to assess the differentiation of MC3T3-E1 cells. **Figure 12** shows that on both cp-Ti and SLA-Ti surfaces, the conditioned medium achieved from RAW264.7 cells incubated on titanium surfaces preserved in 10 and 100 μM naringin-containing solution showed a better osteogenic ability to MC3T3-E1 cells compared with other groups. It indicated that 10 and 100 μM naringin-containing solution could provide a better osteoimmune microenvironment.

DISCUSSION

In this study, we evaluated the effect of saline solution containing naringin on the surface characteristics and biocompatibility of cp-Ti and SLA-Ti stored for 4 weeks. Our results clearly revealed that titanium preserved in solution reduced hydrocarbon contamination and increased hydrophilicity. Samples preserved in 10 μM naringin-containing solution significantly promoted osteoblast adhesion, proliferation, and differentiation. Moreover, the naringin crystals absorbed on the surfaces exhibited an anti-inflammatory effect by suppressing the NF-κB signal pathway. Certain concentration of naringin-containing solution could form a favorable osteoimmune microenvironment.

SEM images indicated that the substantive characteristics of cp-Ti had no connection with the storage methods. However, the SLA-Ti preserved in liquid could be observed in nanostructures on surfaces after 4 weeks. This phenomenon corresponded with some previous research (Shen et al., 2016; Choi et al., 2019). Wennerberg et al. demonstrated that titanium plates undergo acid etching and are kept in solution as necessary conditions for the formation of nanostructures. A possible hypothesis of this phenomenon may be the reorganization of the outermost titanium oxide layer. The hydride layers formed by etching act as nucleation centers, the dissociative adsorption of water, and Ti diffusion contribute to the growth of the nanostructure. This kind of morphological enhanced differentiation of osteoblasts and affected osteointegration (Wennerberg et al., 2013; Ghassemi et al., 2018). The Raman test demonstrated the existence of naringin crystals on titanium surfaces after 4 weeks' storage in naringin-containing solution. Optical profiler analysis showed no differences in surface roughness in cp-Ti and SLA-Ti groups. It was consistent with the conclusion of several studies that liquid storage would not significantly alter implant roughness (Lu et al., 2012).

XPS tests showed that the carbon levels of samples preserved in aqueous solution were lower than that exposed to air for both cp-Ti and SLA-Ti. It may have to do with the liquid isolating hydrocarbons in the air from contacting with the titanium surface. The carbon levels of titanium disks soaked in 100 μM and 1 mM naringin-containing solution increased gradually compared with the 0.9% Nacl and 10 μM naringin-containing group. It may contribute to the naringin crystals adsorbed on the titanium surface that increase with the concentration of naringin-containing solution. The hydrocarbon contamination on titanium surfaces is related to the wettability and the behaviors of osteoblasts (Hayashi et al., 2014).

Hydrophilicity is an important physicochemical characteristic of titanium implant surfaces. Although hydrophilicity is not the decisive factor affecting the biological activity of implants (Aita et al., 2009), studies have demonstrated that compared to SLA surfaces, SLActive surfaces displayed better osteointegration ability and showed the capacity of regulating the polarization of macrophages (Donos et al., 2011; Hotchkiss et al., 2016). Surfaces preserved in solution exhibited better wettability compared to surfaces exposed to air. It may be related to lower carbon contents of liquid stored titanium. In addition, the titanium disks soaked in naringin-containing solution showed better hydrophilicity than samples preserved in saline. This may contribute to competitive adsorption of storage solution, solute, and hydrocarbon on titanium surface. We hypothesized that naringin crystals could compete for hydrocarbon adsorption sites, thus reducing the adsorption of hydrocarbons on the surface of titanium and increasing the hydrophilicity.

Biocompatibility studies were performed to evaluate the biocompatibility of titanium surfaces under different storage methods. As previously reported, saline storage can improve the physiochemical characteristics and promote bioactivity of implants, which was in accord with the results of the present study (Tang K. M. et al., 2021). It can be attributed to the

reduction of carbon contamination on implant surfaces. Previous studies showed that carbon deposition might decrease the expression of vinculin in osteoblasts, which played a crucial role in cell adhesion (Hayashi et al., 2014).Moreover, carbon contamination could change the electrostatic status of titanium surfaces. The new titanium surface is electropositive and can bind directly to negatively charged proteins and cells. However, hydrocarbon contamination may change the electric charges on aged titanium surfaces, resulting in a decrease of biological activities (Att et al., 2009b; Hayashi et al., 2014). Especially on SLA-Ti surfaces, nanostructures formed after preserving in aqueous solution for 4 weeks, which is beneficial for proliferation, sketching, and differentiation of osteoblasts. In this study, cells on 10 μM naringin-containing solution stored titanium stretched out more and longer pseudopodia in cell morphological observation. No cytotoxicity of cp-Ti and SLA-Ti preserved in three different concentrations of naringin-containing solution was observed. In addition, the naringin storage solution significantly promoted the proliferation of MC3T3-E1 cells after culturing for 7 days. Western blot analysis and qRT-PCR analysis confirmed that the expression of osteogenic proteins and mRNAs under the 10 μM naringin-containing solution storage method were up-regulated, indicating good biocompatibility. This may be due to the pharmacological effects of naringin, which was adsorbed to the surface of titanium. Naringin can exert biological activity in a certain concentration range. Shao et al. designed naringin-loaded rutile nanorod films and detected that naringin played an important role in the adhesion, proliferation, and mineralization of MSCs (Shao et al., 2019). Wu et al. detected that 0.3–10 μM naringin can stimulate BMP-2 expression of MC3T3-E1 cells, and the most effective concentrations were 3 μM (Wu et al., 2008). It has been reported that naringin could enhance the proliferation and differentiation of MG-63 cells in a concentration-dependent manner (1–100 μg/ml). When the concentrations were 1 and 10 μg/ml, MG-63 cells displayed the best osteogenic properties (Chen et al., 2013). However, high concentrations of naringin have a detrimental effect on cells. Yin et al. detected that 1 μM amount of naringin had the best performance in the proliferation and osteogenic differentiation of hPDLSCs *in vitro* and *in vivo*. However, when the concentration of naringin was up to 100 μM, the proliferation of hPDLSCs was inhibited (Yin et al., 2015). When the concentration of naringin was greater than 200 μg/ml, it may cause the death of MSCs (Zhang et al., 2009). Therefore, naringin solution with concentration ranging from 10 μM to 1 mM was selected in this experiment.

After implantation, the body's immune response can be induced. Macrophages are essential elements of the immune system. The surface properties of implants have been proved to modulate the behaviors of macrophages (Zhang et al., 2019). Macrophages participate in the regulation of the bone healing process by secreting a variety of cytokines. Studies showed that hydrophilic surfaces induced the decrease of pro-inflammatory cytokine gene levels (Alfarsi et al., 2014; Abaricia et al., 2020), which is also proved in our study. In addition, naringin-containing solution stored samples further reduced the inflammatory response of macrophages. This phenomenon may attribute to the anti-inflammatory property of naringin crystals. The results of the present study indicated that 10 and 100 μM naringin-containing solution exhibited excellent anti-inflammatory effects.

NF-κB is an important transcriptional factor involved in tumor, inflammation, and immunity (Mitchell et al., 2016). It can control the expression of pro-inflammatory genes to modulate inflammatory responses (Mitchell and Carmody, 2018). In normal cells, NF-κB exists in the form of inactivated p50/p65/IκBα. After activation of the NF-κB signal pathway, IκBα was phosphorylated and dissociated from the p50/p65/IκBα complex. Subsequently, p65 was phosphorylated and activated. After nuclear translocation, p-p65 could bind to the promoter region of the target gene to stimulate the transcription of the target gene and exert its biological effect (Oeckinghaus et al., 2011). The NF-κB signaling pathway plays a role in the anti-inflammatory effects of naringin (Zhao et al., 2016). According to the present results, ratios of p-p65/p65 and p-IκBα/IκBα were significantly decreased in 10 and 100 μM NAR groups, indicating that the NF-kB pathway was inhibited by certain concentrations of naringin.

The concept of osteoimmunology has been proposed to describe the close relationship between the skeletal system and the immune system (Arron and Choi, 2000). Bone cells and immune cells share the same microenvironment and interact with each other. A dental implant can be detected by immune system as a foreign body and trigger immune responses, which influence the behaviors of osteoblasts and osteoclasts. Therefore, satisfactory osseointegration is the result of the interaction of multiple systems (Chen Z. et al., 2016). In the present study, the osteogenic differentiation ability of MC3T3-E1 cells in the conditioned media was examined to investigate the influence of the immune system. We found 10 and 100 μM naringin-containing solutions had the best performance in regulating the immune microenvironment and thus promoting the differentiation of MC3T3-E1 cells.

However, there are several limitations of this study that should be taken into account when interpreting these data. The dimensions and shape of titanium samples used in this study are not consistent with the implant used in clinics. It would be better to perform vivo experiments to further validate the results of the present study. We used murine MC3T3-E1 osteoblasts rather than human isolated cells. Although species difference exists, cell lines have the advantages of unlimited cell number, easy access, and homogenous character (Czekanska et al., 2012). The murine RAW264.7 cell line is generally used to construct inflammatory models and study inflammatory responses (Liu et al., 2018). Although there are some limitations, according to the results of the current experiment, a normal saline solution containing 10 μM naringin had a positive effect on titanium surfaces, so as to provide new ideas and new directions for clinical implant storage.

CONCLUSION

In conclusion, we developed a new naringin-containing solution to store different kinds of titanium implants in this study. The results

demonstrated that after storing titanium surfaces under different conditions for 4 weeks, 10 μM naringin-containing solution stored samples displayed lower carbon contamination levels and better hydrophilicity. At the same time, 10 μM naringin-containing solution stored samples exhibited excellent osteogenic properties, anti-inflammatory, and immunomodulatory ability. The 10 μM naringin-containing solution method was proven to be an effective new storage condition.

DATA AVAILABILITY STATEMENT

The raw data supporting the conclusions of this article will be made available by the authors, without undue reservation.

AUTHOR CONTRIBUTIONS

WC contributed to the design, data acquisition, and analysis and drafted the manuscript. W-QZ contributed to the design and data analysis. SS and YL contributed to data acquisition. The corresponding author JQ contributed to the conception, design, data interpretation, and critically revised the manuscript. All authors agreed to be accountable for all aspects of the work. All authors have read and agreed to the published version of the manuscript.

FUNDING

We declare all sources of funding received for the research being submitted. This work was supported by the National Natural Science Foundation of China (Project Number: 81870799), the Jiangsu Provincial Key Research and Development Program (Project Number: BE2019728), the Nanjing Medical University-SUYAN Group Intelligent Innovation Research and Development Project (Project Number: NMU-SY201806), the Southeast University-Nanjing Medical University Cooperative Research Project (Project Number: 2242017K3DN14), and the Foundation of Priority Academic Program Development of Jiangsu Higher Education Institutions (Project Number: 2018-87).

REFERENCES

Abaricia, J. O., Shah, A. H., Musselman, R. M., and Olivares-Navarrete, R. (2020). Hydrophilic Titanium Surfaces Reduce Neutrophil Inflammatory Response and Netosis. *Biomater. Sci.* 8 (8), 2289–2299. doi:10.1039/c9bm01474h

Aita, H., Hori, N., Takeuchi, M., Suzuki, T., Yamada, M., Anpo, M., et al. (2009). The Effect of Ultraviolet Functionalization of Titanium on Integration with Bone. *Biomaterials* 30 (6), 1015–1025. doi:10.1016/j.biomaterials.2008.11.004

Alam, M. A., Subhan, N., Rahman, M. M., Uddin, S. J., Reza, H. M., and Sarker, S. D. (2014). Effect of Citrus Flavonoids, Naringin, and Naringenin, on Metabolic Syndrome and Their Mechanisms of Action. *Adv. Nutr.* 5 (4), 404–417. doi:10.3945/an.113.005603

Alfarsi, M. A., Hamlet, S. M., and Ivanovski, S. (2014). Titanium Surface Hydrophilicity Modulates the Human Macrophage Inflammatory Cytokine Response. *J. Biomed. Mater. Res.* 102 (1), 60–67. doi:10.1002/jbm.a.34666

Arron, J. R., and Choi, Y. (2000). Bone versus Immune System. *Nature* 408 (6812), 535–536. doi:10.1038/35046196

Att, W., and Ogawa, T. (2012). Biological Aging of Implant Surfaces and Their Restoration with Ultraviolet Light Treatment: A Novel Understanding of Osseointegration. *Int. J. Oral Maxillofac. Implants* 27 (4), 753–761.

Att, W., Hori, N., Iwasa, F., Yamada, M., Ueno, T., and Ogawa, T. (2009a). The Effect of Uv-Photofunctionalization on the Time-Related Bioactivity of Titanium and Chromium-Cobalt Alloys. *Biomaterials* 30 (26), 4268–4276. doi:10.1016/j.biomaterials.2009.04.048

Att, W., Hori, N., Takeuchi, M., Ouyang, J., Yang, Y., Anpo, M., et al. (2009b). Time-Dependent Degradation of Titanium Osteoconductivity: An Implication of Biological Aging of Implant Materials. *Biomaterials* 30 (29), 5352–5363. doi:10.1016/j.biomaterials.2009.06.040

Bosshardt, D. D., Chappuis, V., and Buser, D. (2017). Osseointegration of Titanium, Titanium Alloy, and Zirconia Dental Implants: Current Knowledge and Open Questions. *Periodontol. 2000* 73 (1), 22–40. doi:10.1111/prd.12179

Buser, D., Broggini, N., Wieland, M., Schenk, R. K., Denzer, A. J., Cochran, D. L., et al. (2004). Enhanced Bone Apposition to a Chemically Modified Sla Titanium Surface. *J. Dent Res.* 83 (7), 529–533. doi:10.1177/154405910408300704

Chen, K.-Y., Lin, K.-C., Chen, Y.-S., and Yao, C.-H. (2013). A Novel Porous Gelatin Composite Containing Naringin for Bone Repair. *Evidence-Based Complement. Altern. Med.* 2013, 1–10. doi:10.1155/2013/283941

Chen, R., Qi, Q.-L., Wang, M.-T., and Li, Q.-Y. (2016a). Therapeutic Potential of Naringin: An Overview. *Pharm. Biol.* 54 (12), 3203–3210. doi:10.1080/13880209.2016.1216131

Chen, Z., Klein, T., Murray, R. Z., Crawford, R., Chang, J., Wu, C., et al. (2016b). Osteoimmunomodulation for the Development of Advanced Bone Biomaterials. *Mater. Today* 19 (6), 304–321. doi:10.1016/j.mattod.2015.11.004

Choi, S.-H., Jeong, W.-S., Cha, J.-Y., Lee, J.-H., Lee, K.-J., Yu, H.-S., et al. (2017). Effect of the Ultraviolet Light Treatment and Storage Methods on the Biological Activity of a Titanium Implant Surface. *Dental Mater.* 33 (12), 1426–1435. doi:10.1016/j.dental.2017.09.017

Choi, S.-H., Ryu, J.-H., Kwon, J.-S., Kim, J.-E., Cha, J.-Y., Lee, K.-J., et al. (2019). Effect of Wet Storage on the Bioactivity of Ultraviolet Light- and Non-Thermal Atmospheric Pressure Plasma-Treated Titanium and Zirconia Implant Surfaces. *Mater. Sci. Eng. C* 105, 110049. doi:10.1016/j.msec.2019.110049

Czekanska, E., Stoddart, M. J., Stoddart, M., Richards, R., and Hayes, J. (2012). In Search of an Osteoblast Cell Model for *In Vitro* Research. *eCM* 24, 1–17. doi:10.22203/ecm.v024a01

Donos, N., Hamlet, S., Lang, N. P., Salvi, G. E., Huynh-Ba, G., Bosshardt, D. D., et al. (2011). Gene Expression Profile of Osseointegration of a Hydrophilic Compared with a Hydrophobic Microrough Implant Surface. *Clin. Oral Implants Res.* 22 (4), 365–372. doi:10.1111/j.1600-0501.2010.02113.x

Ghassemi, A., Ishijima, M., Hasegawa, M., Mohammadzadeh Rezaei, N., Nakhaei, K., Sekiya, T., et al. (2018). Biological and Physicochemical Characteristics of 2 Different Hydrophilic Surfaces Created by Saline-Storage and Ultraviolet Treatment. *Implant Dent.* 27 (4), 405–414. doi:10.1097/id.0000000000000773

Hamlet, S., Alfarsi, M., George, R., and Ivanovski, S. (2012). The Effect of Hydrophilic Titanium Surface Modification on Macrophage Inflammatory Cytokine Gene Expression. *Clin. Oral Impl. Res.* 23 (5), 584–590. doi:10.1111/j.1600-0501.2011.02325.x

Hayashi, R., Ueno, T., Migita, S., Tsutsumi, Y., Doi, H., Ogawa, T., et al. (2014). Hydrocarbon Deposition Attenuates Osteoblast Activity on Titanium. *J. Dent. Res.* 93 (7), 698–703. doi:10.1177/0022034514536578

Hori, N., Att, W., Ueno, T., Sato, N., Yamada, M., Saruwatari, L., et al. (2009). Age-Dependent Degradation of the Protein Adsorption Capacity of Titanium. *J. Dent. Res.* 88 (7), 663–667. doi:10.1177/0022034509339567

Hotchkiss, K. M., Reddy, G. B., Hyzy, S. L., Schwartz, Z., Boyan, B. D., and Olivares-Navarrete, R. (2016). Titanium Surface Characteristics, Including Topography and Wettability, Alter Macrophage Activation. *Acta Biomater.* 31, 425–434. doi:10.1016/j.actbio.2015.12.003

Kasemo, B., and Lausmaa, J. (1988). Biomaterial and Implant Surfaces: On the Role of Cleanliness, Contamination, and Preparation Procedures. *J. Biomed. Mater. Res.* 22 (A2 Suppl. l), 145–158. doi:10.1002/jbm.820221307

Lavrador, P., Gaspar, V. M., and Mano, J. F. (2018). Bioinspired Bone Therapies Using Naringin: Applications and Advances. *Drug Discov. Today* 23 (6), 1293–1304. doi:10.1016/j.drudis.2018.05.012

Lee, J. H., and Ogawa, T. (2012). The Biological Aging of Titanium Implants. *Implant Dent.* 21 (5), 415–421. doi:10.1097/ID.0b013e31826a51f4

Liu, W., Zhang, Y., Zhu, W., Ma, C., Ruan, J., Long, H., et al. (2018). Sinomenine Inhibits the Progression of Rheumatoid Arthritis by Regulating the Secretion of Inflammatory Cytokines and Monocyte/Macrophage Subsets. *Front. Immunol.* 9, 2228. doi:10.3389/fimmu.2018.02228

Lotz, E. M., Olivares-Navarrete, R., Hyzy, S. L., Berner, S., Schwartz, Z., and Boyan, B. D. (2017). Comparable Responses of Osteoblast Lineage Cells to Microstructured Hydrophilic Titanium-Zirconium and Microstructured Hydrophilic Titanium. *Clin. Oral Impl. Res.* 28 (7), e51–e59. doi:10.1111/clr.12855

Lu, H., Zhou, L., Wan, L., Li, S., Rong, M., and Guo, Z. (2012). Effects of Storage Methods on Time-Related Changes of Titanium Surface Properties and Cellular Response. *Biomed. Mater.* 7 (5), 055002. doi:10.1088/1748-6041/7/5/055002

Marconi, G. D., Diomede, F., Pizzicannella, J., Fonticoli, L., Merciaro, I., Pierdomenico, S. D., et al. (2020). Enhanced Vegf/Vegf-R and Runx2 Expression in Human Periodontal Ligament Stem Cells Cultured on Sandblasted/Etched Titanium Disk. *Front. Cel Dev. Biol.* 8, 315. doi:10.3389/fcell.2020.00315

Marconi, G. D., Fonticoli, L., Della Rocca, Y., Oliva, S., Rajan, T. S., Trubiani, O., et al. (2021). Enhanced Extracellular Matrix Deposition on Titanium Implant Surfaces: Cellular and Molecular Evidences. *Biomedicines* 9 (11), 1710. doi:10.3390/biomedicines9111710

Massaro, C., Rotolo, P., De Riccardis, F., Milella, E., Napoli, A., Wieland, M., et al. (2002). Comparative Investigation of the Surface Properties of Commercial Titanium Dental Implants. Part I: Chemical Composition. *J. Mater. Sci. Mater. Med.* 13 (6), 535–548. doi:10.1023/a:1015170625506

Mijiritsky, E., Lorean, A., Mazor, Z., and Levin, L. (2015). Implant Tooth-Supported Removable Partial Denture with at Least 15-Year Long-Term Follow-Up. *Clin. Implant Dent. Relat. Res.* 17 (5), 917–922. doi:10.1111/cid.12190

Miles, E. A., and Calder, P. C. (2021). Effects of Citrus Fruit Juices and Their Bioactive Components on Inflammation and Immunity: A Narrative Review. *Front. Immunol.* 12, 712608. doi:10.3389/fimmu.2021.712608

Minamikawa, H., Att, W., Ikeda, T., Hirota, M., and Ogawa, T. (2016). Long-Term Progressive Degradation of the Biological Capability of Titanium. *Materials* 9 (2), 102. doi:10.3390/ma9020102

Mitchell, J. P., and Carmody, R. J. (2018). NF-κB and the Transcriptional Control of Inflammation. *Int. Rev. Cel Mol. Biol.* 335, 41–84. doi:10.1016/bs.ircmb.2017.07.007

Mitchell, S., Vargas, J., and Hoffmann, A. (2016). Signaling via the NFκB System. *Wires Syst. Biol. Med.* 8 (3), 227–241. doi:10.1002/wsbm.1331

Oeckinghaus, A., Hayden, M. S., and Ghosh, S. (2011). Crosstalk in NF-κB Signaling Pathways. *Nat. Immunol.* 12 (8), 695–708. doi:10.1038/ni.2065

Ping, J., Zhou, C., Dong, Y., Wu, X., Huang, X., Sun, B., et al. (2021). Modulating Immune Microenvironment during Bone Repair Using Biomaterials: Focusing on the Role of Macrophages. *Mol. Immunol.* 138, 110–120. doi:10.1016/j.molimm.2021.08.003

Prasad, S., Ehrensberger, M., Gibson, M. P., Kim, H., and Monaco, E. A. (2015). Biomaterial Properties of Titanium in Dentistry. *J. Oral Biosci.* 57 (4), 192–199. doi:10.1016/j.job.2015.08.001

Shao, Y., You, D., Lou, Y., Li, J., Ying, B., Cheng, K., et al. (2019). Controlled Release of Naringin in Gelma-Incorporated Rutile Nanorod Films to Regulate Osteogenic Differentiation of Mesenchymal Stem Cells. *ACS Omega* 4 (21), 19350–19357. doi:10.1021/acsomega.9b02751

Shen, J.-W., Chen, Y., Yang, G.-L., Wang, X.-X., He, F.-M., and Wang, H.-M. (2016). Effects of Storage Medium and Uv Photofunctionalization on Time-Related Changes of Titanium Surface Characteristics and Biocompatibility. *J. Biomed. Mater. Res.* 104 (5), 932–940. doi:10.1002/jbm.b.33437

Shen, K., Zhang, X., Tang, Q., Fang, X., Zhang, C., Zhu, Z., et al. (2021). Microstructured Titanium Functionalized by Naringin Inserted Multilayers for Promoting Osteogenesis and Inhibiting Osteoclastogenesis. *J. Biomater. Sci. Polym. Ed.* 32 (14), 1865–1881. doi:10.1080/09205063.2021.1949098

Suzuki, T., Hori, N., Att, W., Kubo, K., Iwasa, F., Ueno, T., et al. (2009). Ultraviolet Treatment Overcomes Time-Related Degrading Bioactivity of Titanium. *Tissue Eng. A* 15 (12), 3679–3688. doi:10.1089/ten.TEA.2008.0568

Tang, K. M., Zhang, W.-S., Liu, Y., Zhu, W.-Q., and Qiu, J. (2021a). Physicochemical Properties and *In Vitro* Osteocompatibility of Different Titanium Surfaces Stored in a Saline Solution. *Mater. Res. Express* 8, 065403. doi:10.1088/2053-1591/ac0a04

Tang, Z. H., Su, S., Liu, Y., Zhu, W.-q., Zhang, S.-m., and Qiu, J. (2021b). Hydrothermal Synthesis of Zinc-Incorporated Nano-Cluster Structure on Titanium Surface to Promote Osteogenic Differentiation of Osteoblasts and hMSCs. *Front. Mater.* 8 (363), 739071. doi:10.3389/fmats.2021.739071

Wennerberg, A., Svanborg, L. M., Berner, S., and Andersson, M. (2013). Spontaneously Formed Nanostructures on Titanium Surfaces. *Clin. Oral Impl. Res.* 24 (2), 203–209. doi:10.1111/j.1600-0501.2012.02429.x

Wu, J.-B., Fong, Y.-C., Tsai, H.-Y., Chen, Y.-F., Tsuzuki, M., and Tang, C.-H. (2008). Naringin-Induced Bone Morphogenetic Protein-2 Expression via Pi3k, Akt, C-Fos/C-Jun and Ap-1 Pathway in Osteoblasts. *Eur. J. Pharmacol.* 588 (2-3), 333–341. doi:10.1016/j.ejphar.2008.04.030

Yin, L., Cheng, W., Qin, Z., Yu, H., Yu, Z., Zhong, M., et al. (2015). Effects of Naringin on Proliferation and Osteogenic Differentiation of Human Periodontal Ligament Stem Cells *In Vitro* and *In Vivo*. *Stem Cell Int.* 2015, 1–9. doi:10.1155/2015/758706

Yu, M., You, D., Zhuang, J., Lin, S., Dong, L., Weng, S., et al. (2017). Controlled Release of Naringin in Metal-Organic Framework-Loaded Mineralized Collagen Coating to Simultaneously Enhance Osseointegration and Antibacterial Activity. *ACS Appl. Mater. Inter.* 9 (23), 19698–19705. doi:10.1021/acsami.7b05296

Zhang, P., Dai, K.-r., Yan, S.-g., Yan, W.-q., Chao-Zhang, C., Chen, D.-q., et al. (2009). Effects of Naringin on the Proliferation and Osteogenic Differentiation of Human Bone Mesenchymal Stem Cell. *Eur. J. Pharmacol.* 607 (1-3), 1–5. doi:10.1016/j.ejphar.2009.01.035

Zhang, Y., Cheng, X., Jansen, J. A., Yang, F., and van den Beucken, J. J. J. P. (2019). Titanium Surfaces Characteristics Modulate Macrophage Polarization. *Mater. Sci. Eng. C* 95, 143–151. doi:10.1016/j.msec.2018.10.065

Zhao, Y. D., Gao, Y., Yue, J., Ding, X. L., Deng, Y., Du, B., et al. (2015). Effect of Argon Protection on the Biological Activity of Acid Etched Titanium Surface. *Eur. Rev. Med. Pharmacol. Sci.* 19 (9), 1568–1576.

Zhao, Y., Li, Z., Wang, W., Zhang, H., Chen, J., Su, P., et al. (2016). Naringin Protects against Cartilage Destruction in Osteoarthritis through Repression of NF-κB Signaling Pathway. *Inflammation* 39 (1), 385–392. doi:10.1007/s10753-015-0260-8

Conflict of Interest: The authors declare that the research was conducted in the absence of any commercial or financial relationships that could be construed as a potential conflict of interest.

Publisher's Note: All claims expressed in this article are solely those of the authors and do not necessarily represent those of their affiliated organizations, or those of the publisher, the editors, and the reviewers. Any product that may be evaluated in this article, or claim that may be made by its manufacturer, is not guaranteed or endorsed by the publisher.